decay of the gamma-ray activity excited by neutron bombardment. It is apparent that there are gamma-ray periods for the 13-second and 54-minute activities. The energy of each of these has not yet been determined. The energies of the upper limits of the beta-radiations from the 54-minute and 13-second activities have been reported[7] as 1.3 Mev and 3.2 Mev, respectively. In the present investigation about 750 tracks have been measured for the 50-day period and about 100 tracks for the positive 20-minute period. These measurements indicate energies at the upper limit of 2.15 Mev and 1.75 Mev, respectively. Measurements are in progress to determine as far as possible the beta- and gamma-energies for the remaining activities.

We are greatly indebted to Mr. D. W. Stewart for aid in carrying out the necessary chemical separations.

The work has been made possible by a grant from the Horace H. Rackham Trust Fund.

[7] Gaerttner, Turin and Crane, Phys. Rev. **49**, 793 (1937).

SEPTEMBER 15, 1937 PHYSICAL REVIEW VOLUME 52

The Magnetic Moment of the Proton

I. ESTERMANN, O. C. SIMPSON AND O. STERN
Research Laboratory of Molecular Physics, Carnegie Institute of Technology, Pittsburgh, Pennsylvania

(Received July 9, 1937)

The magnetic moment of the proton was measured by the method of the magnetic deflection of molecular beams employing H_2 and HD. The result is $\mu_P = 2.46\mu_0 \pm 3$ percent.

THE magnetic moment of the proton was first measured by Estermann, Frisch and Stern in Hamburg in 1932–33.[1] These measurements gave the surprising result that the proton moment was not one but 2.5 nuclear magnetons with the limit of error of about 10 percent. We have repeated these measurements with the aim of obtaining as great an accuracy as possible. The knowledge of this numerical value is important for several reasons: It allows a check on any theory of the heavy elementary particles, because the theory must give just this numerical value; but it is, of course, also important for the theory of the nuclei and for the theory of the forces between elementary particles.

In addition to the experiments with H_2, we have employed beams of HD[2] and have removed certain sources of error contained in the previous measurements.

I. METHOD

The principle of the method used is the measurement of the deflection of a beam of hydrogen molecules in an inhomogeneous magnetic field. From this measurement the magnetic moment of the proton is obtained in the following way:

Normal hydrogen is composed of 25 percent parahydrogen and 75 percent orthohydrogen. We neglect, at first, the rotation of the molecule. Then in the case of parahydrogen, the two proton spins are antiparallel and the total spin and magnetic moment of the molecule are consequently 0. In the case of orthohydrogen, the two proton spins are parallel, resulting in a total spin of the molecule of 1 and a magnetic moment of twice the proton moment. An infinitely narrow beam of orthohydrogen molecules of a definite velocity should, therefore, be split by the magnetic field into three components corresponding to the deflections 0, $+2s_P$ (H_2) and $-2s_P$ (H_2), where s_P (H_2) would be the deflection under the conditions of our experiment of a H_2 molecule having one proton moment. A beam of parahydrogen would give only the one undeflected component.

In addition to this splitting due to the magnetic moment of the protons, we have to consider the magnetic moment due to the rotation of the molecule as a whole. At very low temperatures all the parahydrogen molecules have the

[1] R. Frisch and O. Stern, Zeits. f. Physik **85**, 4 (1933); U. z. M. 24; I. Estermann and O. Stern, Zeits. f. Physik **85**, 17 (1933); U. z. M. 27. (U. z. M., Untersuchungen zur Molekularstrahlmethode, refers to a series of papers concerning the molecular ray method.)

[2] We wish to express our sincere thanks to Dr. F. G. Brickwedde of the National Bureau of Standards who kindly prepared the HD.

TABLE I. *Distribution of rotational quantum states.*

	l	$T=90°K$	$T=291°K$
ortho-H_2	1	99.98%	88.2%
	3	0.02	11.7
	5		0.1
para-H_2	0	98.3%	51.9%
	2	1.7	46.6
	4		1.5
HD	0	55.5%	20.0%
	1	40.5	39.0
	2	4.0	27.5
	3		10.7
	4		2.4
	5		0.4

rotational state 0, and consequently no rotational magnetic moment; therefore, no magnetic moment at all. This was verified in our Hamburg experiments with pure *para*-H_2 at liquid-air temperature. At room temperature we found a considerable deflection which we ascribed to the rotational moment of the higher quantum states present (see Table I). By further assuming that the rotational magnetic moment is proportional to the rotational quantum number, we found that the rotational magnetic moment per quantum is 0.8 to 0.9 nuclear magnetons.

The orthohydrogen molecules, however, will have the rotational quantum state 1 even at the lowest temperatures. This rotational quantum causes each of the original three components to split again into three, since at the high field strengths used in our experiments the rotational and proton moments can be considered as completely decoupled. The distance between these components is s_R, the deflection of a H_2 molecule having only the magnetic moment associated with the first rotational state, which is about one-third of the proton moment. The total pattern of the orthohydrogen has, thus, nine components, as shown in Fig. 1. Upon adding the 25 percent of the undeflected parahydrogen, we receive the split pattern of ordinary hydrogen at low temperatures. At the temperature of $T=90°K$ where we made measurements, 99.98 percent of the orthohydrogen molecules are in the rotational state $l=1$, and 98.3 percent of the parahydrogen molecules in the rotational state $l=0$ (see Table I). We may therefore neglect the higher rotational states at the temperature of $T=90°K$.

In the case of the HD molecule containing two different atoms, there are no *ortho* and *para* states. At sufficiently low temperatures all the molecules are transformed into the rotational state 0. The experiments, as in the case of H_2, were carried out at $T=90°K$. The distribution of the different rotational states is shown in Table I. Let us consider at first the rotational state 0. In the field strength used we may regard the nuclear magnetic moments of the H and D atoms as completely uncoupled. If the spin and the magnetic moment of the D atom were 0, the deflection pattern of an infinitely narrow monochromatic beam would have just two components $+\frac{1}{2}$ and $-\frac{1}{2}$, because the proton spin is $\frac{1}{2}$. These components correspond to the deflections $\pm s_P$ (HD) of an HD molecule with the magnetic moment of one proton moment. On account of the spin 1 of the D atom, however, each of these components is split into a triplet. The distance between the triplet components is s_D (HD); namely, the deflection of an HD molecule with the magnetic moment of the deuteron. Since the latter moment is only about one-third of the proton moment, s_D (HD) is approximately one-third s_P (HD). For $T=90°K$, 55 percent of the HD molecules are in the state $l=0$, 40 percent in $l=1$ and the rest in $l=2$.

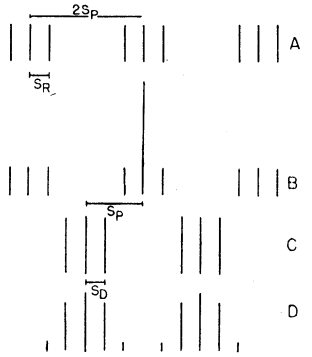

FIG. 1. Magnetic split patterns of H_2 and HD. A, *ortho*-H_2; $T=90°K$. B, normal H_2; $T=90°K$. C, HD without rotation ($l=0$). D, HD; $T=90°K$.

Neglecting state 2, one obtains the split pattern shown in Fig. 1, under the assumption that $s_D=s_R=\frac{1}{3}s_P$. The exact values of s_D and s_R do not matter, because due to the symmetrical arrangement of the s_D and s_R lines around the s_P lines their influence on the intensity distribution

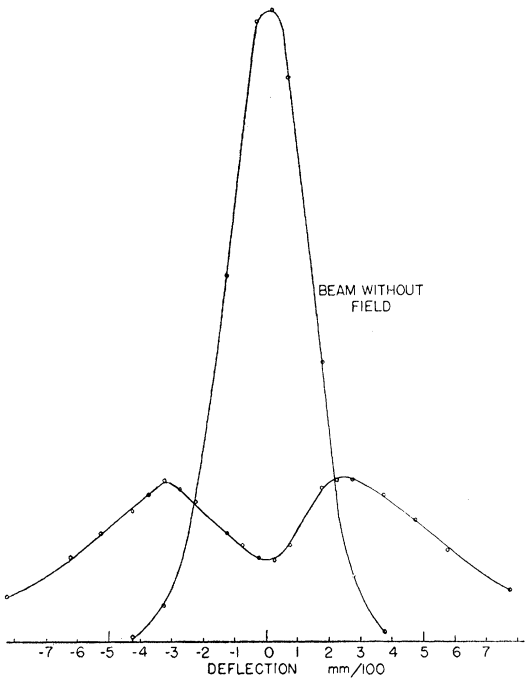

FIG. 2. Magnetic deflection of a beam of HD ($T=90°$K). Intensity in arbitrary units.

of an ordinary nonmonochromatic beam compensates to a large degree.

Actually the experiments were carried out with nonmonochromatic molecular rays of different finite widths in which the molecules have a modified Maxwell distribution of velocities. Each line in Fig. 1 has therefore to be replaced by a Maxwell curve integrated over the finite width of the beam. The actual intensity distribution in the deflected beam is arrived at by superposition of these Maxwell curves.

The characteristic difference in the deflection patterns of H_2 and HD is the absence of a zero beam in the case of HD. With a narrow beam of HD, we receive therefore a deflection curve with a conspicuous minimum in the center (see Fig. 2), in contrast to the H_2 curve (Fig. 3) with a strong maximum in the center.

It should be possible in principle to calculate the unknowns s_P, s_R and s_D from the intensity distribution measured in the experiment. Since the deflection curves, however, are rather insensitive to the value of s_D and s_R, this would be impractical. Being chiefly interested in the moment of the proton, and knowing s_R and s_D from separate experiments with pure parahydrogen and deuterium, respectively, we can calculate s_P from the measured intensity at any point of the deflection curve on the basis of the Maxwell distribution of velocities. $s_P{}^\alpha$ refers then to the deflection of a molecule of the most probable velocity α corresponding to the beam temperature, and the magnetic moment of one proton.[3] For reasons to be explained later (see Section IV), we have used the intensity of the deflected beam at the center of the undeflected beam. We call the ratio of this intensity I to the intensity I_0 of the undeflected beam the "weakening," I/I_0. Assuming a rectangular form for the intensity distribution of the undeflected beam of the half-width $2a$ (see Fig. 4), and a splitting into two beams, as in the case of the alkalies, $I/I_0=F(s^\alpha/a)$, where $F(x)=(1+x)e^{-x}$.[4] For the split pattern of normal H_2 at 90°K (Fig. 1B),

$$\frac{I}{I_0}=\frac{1}{3}+\frac{1}{6}\left[F\left(\frac{s_R{}^\alpha}{a}\right)+F\left(\frac{2s_P{}^\alpha}{a}\right)+F\left(\frac{2s_P{}^\alpha+s_R{}^\alpha}{a}\right)+F\left(\frac{2s_P{}^\alpha-s_R{}^\alpha}{a}\right)\right].$$

For the actual calculations we have used $s_R=\frac{1}{3}s_P$, so that

$$\frac{I}{I_0}=\frac{1}{3}+\frac{1}{6}\left[F\left(\frac{(1/3)s_P{}^\alpha}{a}\right)+F\left(\frac{2s_P{}^\alpha}{a}\right)+F\left(\frac{(7/3)s_P{}^\alpha}{a}\right)+F\left(\frac{(5/3)s_P{}^\alpha}{a}\right)\right].$$

For the pattern of HD at 90°K (Fig. 1D), we have, taking

$$s_D{}^\alpha=s_R{}^\alpha=\tfrac{1}{3}s_P{}^\alpha,$$

$$\frac{I}{I_0}=\frac{1}{3}\left\{F\left(\frac{s_P{}^\alpha}{a}\right)+0.85\left[F\left(\frac{(2/3)s_P{}^\alpha}{a}\right)+F\left(\frac{(4/3)s_P{}^\alpha}{a}\right)\right]+0.15\left[F\left(\frac{(1/3)s_P{}^\alpha}{a}\right)+F\left(\frac{(5/3)s_P{}^\alpha}{a}\right)\right]\right\}.$$

[3] For any given magnetic moment μ, $s^\alpha=(\mu/4kT)\times(dH/ds)\times l^2$ is independent of the mass of the molecule and is therefore the same for H_2 and HD.

[4] O. Stern, Zeits. f. Physik **41**, 563 (1927); U. z. M. 5.

In order to illustrate the small influence of the rotational moment in the case of H_2, and of the rotational and deuteron moment in the case of HD, we refer to Figs. 5 and 6. Fig. 5 shows I/I_0 for H_2 calculated as a function of the half-width $2a$, with and without consideration of the rotational moment; Fig. 6 shows I/I_0 for HD, first setting s_D and $s_R=\frac{1}{3}s_P$ and secondly, $s_D=s_R=0$. The values, $s_D=s_R=\frac{1}{3}s_P$, are in close agreement with the direct measurements of the deuteron moment and the rotational moment of H_2.[5] Under these assumptions, each value of I/I_0 gives a value of $s_P{}^\alpha$. We want to emphasize again that even a comparatively large error in the values of s_R and s_D would influence the value of s_P only to a negligible extent. From $s_P{}^\alpha$ and the constants of the experiment, we calculate the magnetic moment of the proton.

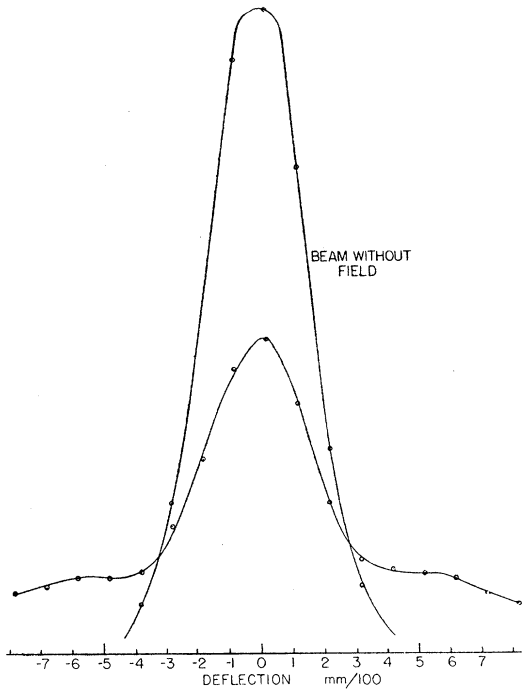

FIG. 3. Magnetic deflection of a beam of H_2 ($T=90°K$). Intensity in arbitrary units.

[5] For the value of the deuteron moment see: I. Estermann and O. Stern; Phys. Rev. **45**, 761 (1934); I. I. Rabi, J. M. B. Kellogg and J. R. Zacharias; Phys. Rev. **45**, 769 (1934); **50**, 472 (1936). There are no direct measurements of the rotational moment of HD. It is to be expected that it is not larger than the rotational moment of H_2. In order to influence our results appreciably, it would have to be of the order of magnitude of the proton moment.

Another series of measurements was made at the beam temperature of 291°K. In this case, the higher rotational states have to be considered (see Table I) and the deflection patterns are more complicated. For H_2 this does not

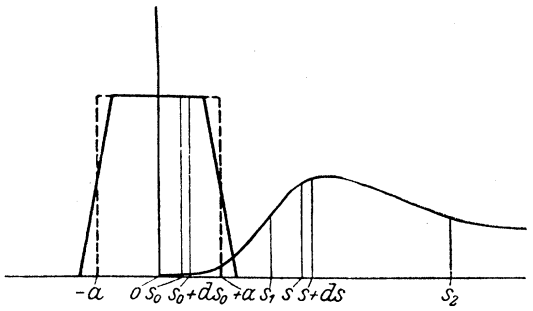

FIG. 4.

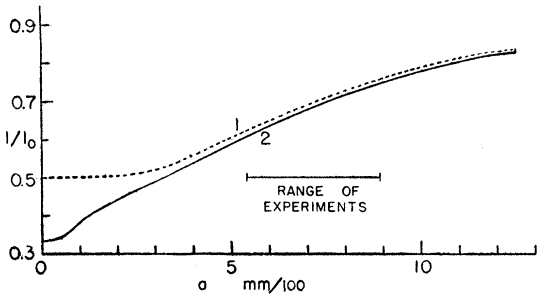

FIG. 5. "Weakening" of a beam of H_2, $T=90°K$; as function of the half-width $2a$. Curve 1, $s_R=0$. Curve 2, $s_R=\frac{1}{3}s_P$.

spoil the correctness of the evaluation of $s_P{}^\alpha$. There are 11 percent of the *ortho*-H_2 molecules in the rotational state $l=3$ and 46 percent of the *para*-H_2 molecules in $l=2$. For the *ortho*-H_2, the influence of the higher temperature is very small, because only one-tenth of the molecules are in a higher rotational state than at liquid-air temperature. For the *para*-H_2, we have directly determined s_R, or rather the "weakening," at room temperature. We were able, therefore, to consider the influence of s_R quite accurately.

For HD, the conditions are less favorable. First, higher rotational quantum states are more populated because of the larger moment of inertia of the HD molecule (see Table I). Secondly, the rotational moment is not so well known (see reference 5). Thirdly, for beams of a width large enough to be employed in our apparatus, the deflection and the weakening are very small, because the effective moment of the

deflected molecules is only about one-half as large as in the case of H_2. For these reasons, we

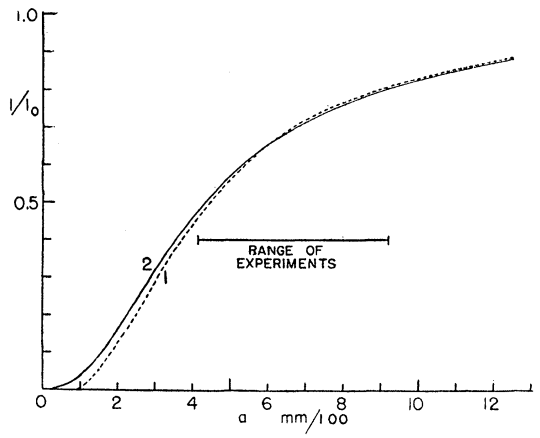

FIG. 6. "Weakening" of a beam of HD, $T=90°K$; as function of the half-width $2a$. Curve 1, $s_R=s_D=0$. Curve 2, $s_R=s_D=\frac{1}{3}s_P$.

have made only one set of measurements with HD at room temperature.

II. EXPERIMENTAL ARRANGEMENT

The apparatus was essentially the same as the one used in the previous measurements in Hamburg. The principle of the arrangement is shown in Fig. 7. A beam of hydrogen molecules formed by the source slit S_1 and the collimating slit S_2 is deflected in an inhomogeneous magnetic field F. The beam intensity is measured by a receiver R which can be moved across the beam. The receiver is a vessel in which the incoming molecules produce a pressure proportional to the intensity of the beam. This pressure is measured by a sensitive hot-wire manometer.

The actual arrangement is shown in Figs. 8 and 9. They are in general self-explanatory, and only remarks about a few details are necessary. The source slit was $\frac{1}{2}$ mm high and 0.02 mm wide, and was fitted with arrangements for alignment and cooling and with a thermocouple. The foreslit was also 0.02 mm wide, and was somewhat higher than the source slit. The collimating slit was formed by two parallel rods mounted on a piece which could be turned from the outside. Thus the width of the beam could be changed during the experiment. A magnetically operated shutter was arranged between the foreslit and collimating slit. The inhomogeneous magnetic field was produced by a pair of pole-pieces of the slot-wedge type, 9.95 cm long; other dimensions as shown in Fig. 10. The height of the beam was limited to about 0.6 mm by a diaphragm at each end of the field.

The receiving manometer is shown in detail in Fig. 11. The receiving slit was a canal 0.5 mm high, 0.02 mm wide, and 3 mm deep. Since the flow resistance of such a canal is very high, the volume of the whole vessel had to be very small to have a reasonable filling time. In our case the volume was 0.6 cm^3, the filling time about $\frac{3}{4}$ minutes. The filament was 9 cm long and was made of 0.001 inch nickel wire from the Driver-Harris Company, and was rolled out in the laboratory shop to a ribbon of 0.085 mm width. With a Wheatstone bridge and a Leeds and Northrup type HS galvanometer, we had a deflection of 155 cm per 10^{-6} mm Hg change in hydrogen pressure. The intensities of the beams used were between 10 and 45 cm deflection. In some experiments, a Kipp and Zonen type Zb galvanometer was used. This instrument was about twice as sensitive, but not very stable.

Further details about the experimental arrangement may be found in the Hamburg papers.

In the measurements with HD, we observed a slight transformation ($2HD=H_2+D_2$) during the experiments. The rate of this decomposition as measured by the weakening of a very narrow beam of HD as a function of time, was found to be about $\frac{1}{2}$ percent per hour. To avoid errors caused by this reaction, we used a fresh supply of HD for each measured weakening.

In agreement with Brickwedde, we found that HD does not decompose if kept in glass vessels

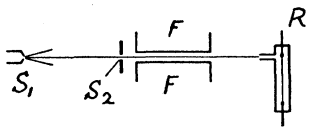

FIG. 7. Schematic diagram of the apparatus. S_1, source slit. S_2, collimating slit. F, magnetic field. R, receiver.

for many months. The decomposition observed during our experiments is probably due to the circulation of the gas through metal diffusion pumps.

III. Inhomogeneity of the Magnetic Field

Since the uncertainty in the inhomogeneity of the magnetic field was one of the major reasons for the larger limit of error in the Hamburg measurements, we have taken great care in the determination of this quantity. The following different methods were used:

(1) The field strength was measured from point to point by means of the change of the electrical resistance of bismuth wires of 1 cm length and 0.1 and 0.15 mm diameter. The wires were moved repeatedly from point to point, using a micrometer slide from the Gaertner Scientific Company, which was accurate to 0.0005 mm. The differences in field strength divided by the displacements gave the inhomogeneity. The measurements were made in the symmetry plane of the field and 0.2 mm above and below; the results are given in Fig. 12.

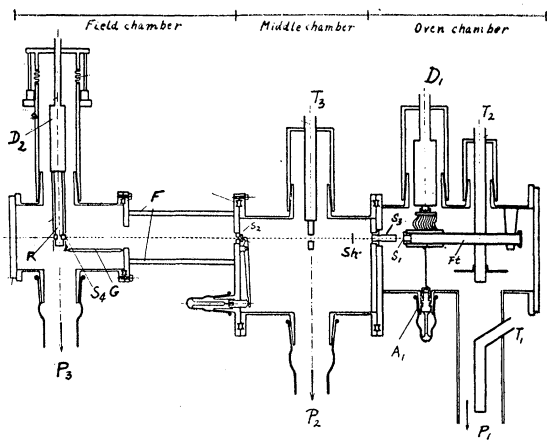

FIG. 8. Vertical cut through the apparatus. P_1, P_2, P_3, pump connections; T_1, T_2, T_3, mercury traps; S_1, source slit; S_2, collimating slit; S_3, foreslit; S_4, receiver slit; D_1, Dewar for cooling of source slit; D_2, Dewar for cooling of manometers R; F, pole-pieces; Sh, shutter; Ft, gas feeding tube; A_1, adjustment screw for vertical displacement of the source slit; G, glass spacer controlling the distance between receiver and pole-pieces.

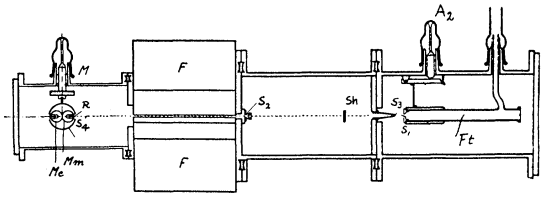

FIG. 9. Horizontal cut through the apparatus. S_1, source slit; S_2, collimating slit; S_3, foreslit; S_4, receiver slit; R, receiver; Ft, gas feeding tube; Sh, shutter; F, pole-pieces; A_2, adjustment screw for the horizontal displacement of the source slit; M, micrometer screw for receiver displacement; Mm, measuring manometer; Mc, compensating manometer.

The bismuth wires were calibrated at six different field strengths of 9380; 13,888; 17,832; 20,330; 21,816 and 22,574 gauss, and at several temperatures by means of an electromagnet with parallel pole-pieces. The values of these standard field strengths were determined with three different flip coils and a ballistic galvanometer which was calibrated by the discharge of a standard capacitance and also with a standard mutual inductance. As a separate check, the field strengths were measured with a magnetic balance. The results obtained by the different flip coil methods agreed within one-half of one percent, and in the average with those measured with the magnetic balance within 2 percent.

(2) A rectangular double flip coil was used for the direct measurement of the inhomogeneity. The coils were made of one turn of copper wire of 0.111 mm diameter and were embedded in paraffin between microscope cover glasses. In this way, the distance between the two flip coils was accurately known (0.138 mm glass plus one wire diameter equals 0.249 mm). Each coil was 37 mm long and 0.207 mm wide (inside between wires). The area of each individual coil was calibrated with the standard field strengths mentioned above. For the measurement of the inhomogeneity, the two coils were connected in series but in opposite directions. If the area of the two coils were exactly the same, their removal from a homogeneous field would produce no deflection of the ballistic galvanometer. In an inhomogeneous field, however, a deflection proportional to the difference of the field strengths at the place of the two coils is obtained. This difference can, therefore, be measured quite accurately; and since the distance between the two coils is known, the inhomogeneity can also be obtained with the same accuracy. In fact, the two flip coils did not have exactly the same area (they were different by 13 percent), but this could be eliminated by taking two series of measurements in which the flip coils were turned by 180°. The flip coil point (see Fig. 12) lies between the two curves but nearer to the curve for the symmetry plane. This is to be expected from the dimensions.

(3) As a final check, we measured the inhomo-

geneity by the ponderomotive force on a bismuth wire which was attached to a quartz fiber, the method used in the previous work.[6] This force is proportional to $H(dH/ds)$, and allows, in connection with the measurement of the field

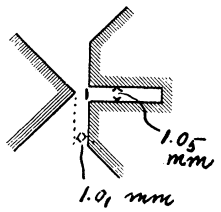

FIG. 10. Cross section of pole-pieces.

strength, the determination of the inhomogeneity. The absolute values of these measurements are not so exact, since the magnetic susceptibility of our bismuth wire was not

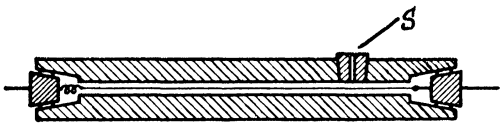

FIG. 11. Manometer. S, receiver slit.

known with great accuracy. This method, however, is very well adapted for relative measurements of the inhomogeneity at different parts of the field. In this respect it agreed very well with the other measurements.

The position of the beam in the field was determined in the following way: A quartz fiber was attached to the front end of the pole-piece with the groove. This quartz fiber causes a shadow in a wide molecular beam. The position of this shadow relative to the center of the beam allows the determination of the distance of the center of the beam from the front end of the pole-piece. In a second experiment the quartz fiber was attached to the rear end of the pole-piece. A similar measurement of the shadow gave the position of the center of the beam when leaving the field. The distances so measured were 0.06 and 0.16 mm. The height of the beam was fixed by a diaphragm on each end of the pole-pieces.

Taking into account the size and position of the beam, and the dimensions of the bismuth wire, we obtain the effective inhomogeneity of 154,000 gauss/cm. We consider this value correct to within less than two percent.

[6] See A. Leu, Zeits. f. Physik **41**, 551 (1927); U. z. M. 4.

IV. Sources of Error and Corrections

The uncertainty of about 10 percent in the previous measurements was due mainly to the fact that the inhomogeneity of the magnetic field (see Section III) and the velocity distribution in the beam were not known accurately enough. It is also necessary to apply a few minor corrections which could be neglected in the previous measurements on account of the larger limit of error.

(a) Velocity distribution

In order to calculate the magnetic moment from the observed intensity in the deflected beam, it is necessary to know the molecular velocities and their distribution. In the previous papers and in Section I, these velocities were calculated on the basis of Maxwell's law from the temperature of the beam. This is not quite correct. The molecular beam does not pass through an absolute vacuum, but through an apparatus which contains a small pressure of hydrogen. This leads to a distortion of the Maxwell distribution. It is to be expected theoretically, and is also supported by experiments, that the slow molecules are scattered more than the fast ones. A molecular beam passing through residual gas shows, therefore, a deficiency of slow molecules compared to Maxwell's law. If we measure the intensity I of the deflected beam as a fraction of the intensity I_0 of the undeflected

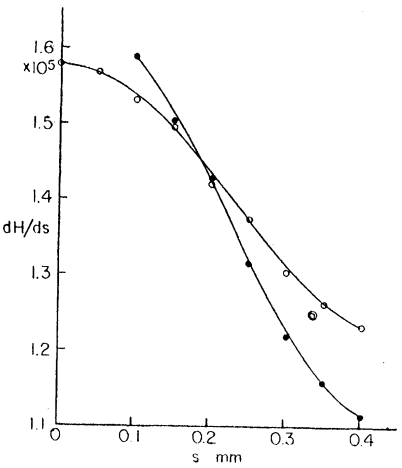

FIG. 12. Inhomogeneity of the field. s, distance from pole-piece fitted with groove. Open circle, points measured in the plane of symmetry. Closed circle, points 0.2 mm above and below the plane of symmetry. Circle within a circle, point measured with double flip coil.

beam, we shall find in the case of small deflections (fast molecules) too large a value; in the case of large deflections (slow molecules) too small a value. It is possible to eliminate this source of

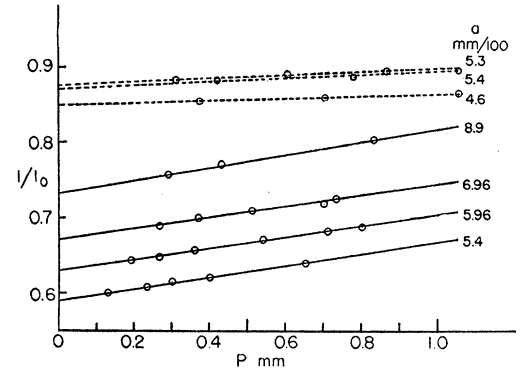

FIG. 13. "Weakening" as function of the scattering pressure for H_2. Full lines, experiments at $T=90°K$. Dotted lines, experiments at $T=291°K$. P, pressure behind the source slit in mm Hg. a, ½ half-width of beam.

error without recourse to special measurements of the scattering by measuring the intensity ratio I/I_0 as a function of the scattering pressure and extrapolating to the pressure 0. Under the obvious assumption that the amount scattered is proportional to the pressure, I/I_0 is, for small pressures, a linear function of the scattering pressure (see appendix). These measurements could be made at any point of the deflected beam, but they are practical only at points where the intensity is large enough. Chiefly for this reason, but also for others mentioned at the end of this section, the measurements used for the final evaluation of the proton moment were those taken at the center of the undeflected beam. We found, in fact, that I/I_0 decreases as a linear function of the scattering pressure, which enabled us to extrapolate safely to the pressure 0 (see Figs. 13 and 14).

The beam passed through three chambers with different scattering pressures (the oven chamber, the middle chamber, and the field chamber, see Fig. 8). We assume that the scattering pressure in all these three rooms is caused by the hydrogen emerging from the source slit, and that the pumping speed at the small pressures in question is constant. Then all the scattering pressures are proportional to each other and proportional to the oven pressure (pressure behind the source slit in the gas reservoir). This was confirmed by direct measurement of the pressures although the very low pressures in the middle and field chamber could not be measured very exactly. Since the oven pressure is the largest of all the pressures involved, it can be measured most accurately. We have plotted I/I_0 as a function of this oven pressure and extrapolated to zero pressure.

It is conceivable that another scattering gas, for instance, mercury vapor, could be present in the apparatus in addition to the scattering hydrogen. If the pressure of this gas were constant, I/I_0 would still be a linear function of pressure, but the curves would be shifted upwards parallel to themselves. The presence of Hg or any other vapor in the apparatus is very unlikely because of the large liquid air cooled surfaces in every part of the apparatus. Furthermore, the presence of such a gas would have a much larger influence on a beam of slow molecules (beam temperature 90°K) than on a beam of fast molecules ($T=291°K$). So if a vapor of constant pressure were present, we would expect to find different values of $s_P{}^\alpha$ from the extrapolated values for different temperatures. A scattering gas of constant pressure should also have a different influence on beams of different widths. No such effects were observed (see Table II).

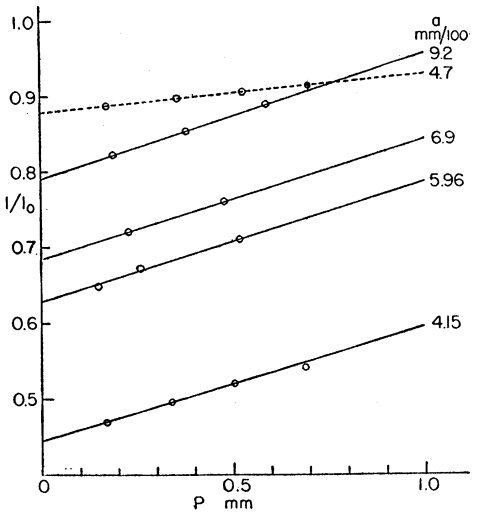

FIG. 14. "Weakening" as function of the scattering pressure for HD. Full lines, experiments at $T=90°K$. Dotted lines, experiments at $T=291°K$. P, pressure behind the source slit in mm Hg. a, ½ half-width of beam.

(b) Other corrections

We have also applied a series of smaller corrections which were omitted in the earlier papers since they were small compared with the uncertainty of 10 percent. With the present accuracy, however, they have to be taken into account.

1. *Form of the undeflected beam.* As stated before, a rectangular intensity distribution of the undeflected beam was assumed as a basis for the calculations. A trapezoid, however, would come much closer to the actual intensity distribution (see Fig. 15). The difference between the calculated results for these two cases is generally less than one percent.

2. *Finite width of the receiver slit.* The measured intensity of the deflected beam in the center of the undeflected beam with a receiver of finite width is the average intensity over the width of the receiver slit (0.02 mm). The difference between this average and the actual intensity at the position $s=0$ is a few tenths of one percent.

3. *Receiver canal.* The receiver is actually not a slit but a canal of 0.02 mm width, 0.5 mm height and 3 mm depth. The alignment of this canal is such that the molecules of the undeflected beam run parallel to its walls (maximum of intensity). The molecules of the deflected beam, however, run obliquely to the walls of the canal; the greater the deflection, the more oblique the path of the molecules. This fact was considered in the previous paper for the intensity measurements of the deflected molecules. It also has, however, an influence on the values of the weakening, but a much smaller one. Since the width of the beam is much larger than the width of the receiver, there are molecules in the deflected beam which hit the receiver at the position $s=0$, but come from the edges of the undeflected beam. For these molecules, the receiver canal is not adjusted correctly and the intensity measured is consequently a little too small (in every case by less than one percent).[7]

4. *Remanent field.* In order to measure the intensity of the undeflected beam a compensation current was sent through the magnet to destroy the remanent field. It was impossible, however, to destroy this field completely, probably because the iron of the pole-pieces had a different remanence at different points. The remaining remanence which could not be destroyed by the compensation current was determined in the following way: The intensity of a helium beam was measured as a function of the width. For wide beams the intensity remained constant. When the beams were made very narrow, the intensity decreased. This was expected for geometrical reasons and for imperfections of slits and alignment. The repetition of these measurements with hydrogen showed a greater decrease of the intensity at narrow beams. The difference in the hydrogen and helium results is apparently due to the deflection of the hydrogen molecules in the remaining remanent field.[8] These measurements were used for computing the inhomogeneity of the remanent field. This correction is only a few tenths of one percent.

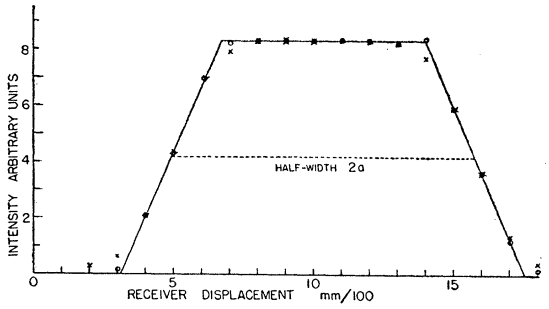

FIG. 15. Form of the undeflected beam. *o*, measured points corrected for finite width of receiver slit. *x*, measured points uncorrected.

(c) Deflected molecules

All these corrections have to be applied also in the case of the "deflected molecules" (points of the deflection curve away from the center). Some of them, however, become rather large and uncertain. At larger deflections, the intensities are so small that the extrapolation of I/I_0 to zero pressure is hardly practical. Correction (3) becomes quite large and consequently the uncertainty about the specular reflection plays a role (see reference 7). Furthermore, the inhomo-

[7] This correction as calculated may be a little too large, because it is derived under the assumption of Knudsen's cosine law; whereas at the small angles involved, a certain amount of specular reflection may occur at the walls of the canal. Since this whole correction is less than one percent, an uncertainty of 10 or even 20 percent is of no importance.

[8] This effect may also be partially due to the diffraction of molecules, since the de Broglie wave-length of H_2 is larger than that of He. The applied correction may, therefore, be a little too large.

geneity changes appreciably along the path of the deflected molecules, and its component in the vertical direction influences the intensity also. In fact, we usually observed an asymmetry in the deflection pattern, which is partly due to these causes, but has probably other experimental reasons as well, since our apparatus was not adapted for a thorough investigation of the deflected molecules. At small deflections, I/I_0 depends very much on the actual form of the undeflected beam, which is not so well defined due to small imperfections of slits and alignment. For all these reasons, the measurements of the deflected molecules could be used only as a rough check, but not for the calculation of an accurate value of the proton moment.

V. Results

The results of the experiments are shown in Table II. $2a$ is the half-width of the beam used. I/I_0 (measured) is the value of the weakening obtained by extrapolation to $p=0$ of the straight lines in Figs. 13 and 14 containing the actually measured points at different pressures. I/I_0 (corrected) is corrected as explained in Section IV. $s_P{}^\alpha$ (90°) is the deflection that a molecule with a magnetic moment of one proton moment and the most probable velocity α corresponding to the temperature of $T=90°$ would have under the conditions of our experiments. The numerical values of $s_P{}^\alpha$ (90°) given in the table are those which lead to the value of the weakening listed under I/I_0 (corrected). The values corresponding to $T=291°$K have been reduced to 90°K by multiplication with the factor 291/90. The two starred runs were made with a different slit alignment at a higher inhomogeneity. The values of $s_P{}^\alpha$ belonging to these runs have been reduced to the standard inhomogeneity.

Table II. *Results of experiments.*

	T	a $\frac{\text{mm}}{100}$	$\frac{I}{I_0}$ (measured)	$\frac{I}{I_0}$ (corrected)	$s_P{}^\alpha$ (90°) $\frac{\text{mm}}{100}$	
H_2	90°	8.90	0.732	0.738	7.65	7.61
H_2	90°	7.00	0.672	0.674	7.59	
H_2	90°	5.96	0.628	0.627	7.72	
H_2	90°	5.40*	0.590	0.587	7.49	
HD	90°	9.20	0.790	0.805	7.37	7.56
HD	90°	6.90	0.684	0.700	7.59	
HD	90°	5.96	0.628	0.645	7.54	
HD	90°	4.15	0.445	0.464	7.76	
H_2	291°	5.40*	0.870	0.879	7.56	7.53
H_2	291°	5.29	0.875	0.885	7.52	
H_2	291°	4.62	0.849	0.861	7.50	
HD	291°	4.70	0.880	0.895	7.82	
				Average	7.59±0.08	

Table III. *Values of the proton moment by different observers.*

Year	Observers	Value Given for the Proton Moment: Mean	Lowest	Highest	Method
1933	F. and S.[1]	2–3	2.	3.	Magnetic deflection of H_2
1933	E. and S.[2]	2.5 ±10%	2.25	2.75	Magnetic deflection of H_2
1934	R., K. and Z.[3]	3.25±10%	2.9	3.6	Magnetic deflection of H
1936	K., R. and Z.[4]	2.85±0.15	2.7	3.0	Magnetic deflection of H
1936	L. and S.[5]	2.3 ±10%	2.07	2.53	Susceptibility of solid hydrogen
		2.7 ±10%	2.43	2.97	
1937	E., S. and S.	2.46±3%	2.38	2.54	Magnetic deflection of H_2 and HD

[1] R. Frisch and O. Stern, Zeits. f. Physik **85**, 4 (1933) (U. z. M. 24).
[2] I. Estermann and O. Stern, Zeits. f. Physik **85**, 17 (1933) (U. z. M. 27).
[3] I. I. Rabi, J. M. B. Kellogg and J. R. Zacharias, Phys. Rev. **46**, 157 (1934).
[4] J. M. B. Kellogg, I. I. Rabi and J. R. Zacharias, Phys. Rev. **50**, 472 (1936).
[5] B. G. Lasarew and L. W. Schubnikow, Physik. Zeits. Sowjetunion **10**, 117 1936), **11**, 445 (1937).

Systematical errors appear to be excluded to a large extent by the close agreement of the measurements under such different conditions (H_2 and HD at 90° and 291°K). Of course, it would be very desirable to check the value of $s_P{}^\alpha$ by measurements of the intensity at larger distances from the center of the beam. Because of the previously mentioned difficulties, we think such experiments could be carried out in the best way with a monochromatic beam.

The averages for $s_P{}^\alpha$ (90°) for the experiments with H_2 at 291°K and 90°K and for HD at 90°K agree within about one percent. The largest deviation from the average is less than three percent. The probable error in the final average of $s_P{}^\alpha$ (90°) $=7.59\times10^{-2}$ mm is 0.08 or 1 percent.

$s_P{}^\alpha$ (90°) allows a calculation of the magnetic moment of the proton μ_P from the equation

$$s_P{}^\alpha=\frac{\mu_P}{4RT}\frac{dH}{ds}l_1{}^2\left(1+2\frac{l_2}{l_1}\right),$$

where $l_1=9.95$ cm is the length of the beam in the field, $l_2=5.03$ cm the distance of the receiver from the end of the field. The temperature T was measured with a thermocouple to better than 1°. $(dH/ds)=154{,}000$ gauss/cm is the effective inhomogeneity. With these values, and a value for

the nuclear magneton of 3.023 c.g.s. units per mole, we obtain for the magnetic moment of the proton

$$\mu_P = 2.46 \text{ nuclear magnetons.}$$

The largest uncertainty (less than 2 percent) is due to the inhomogeneity. $s_P{}^{\alpha}$ and T are accurate to about one percent, while the errors in l_1 and l_2 are negligible. Provided there are no systematical errors, the value of the proton moment should be accurate to within three percent.

A summary of all the published measurements of the magnetic moment of the proton is given in Table III.

The mean value of the proton moment from our new measurements coincides practically with our old Hamburg value. This close agreement is, of course, accidental, considering the limits of error. The values obtained by the method of beams of *atomic* hydrogen are decidedly higher. Although the last measurements with atomic hydrogen come closer to our value, the discrepancy is still outside the limits of error. If this discrepancy were real, it would probably give new information about the interaction between the proton and the electron.[9] It is, however, still possible that the discrepancy is due to imperfections in the experiments. The measurements of the susceptibility of solid hydrogen, which could give an independent check, are at present not quite accurate enough.

We wish to express our gratitude to the Buhl Foundation for financial aid in carrying out the experiments.

[9] L. A. Young, Phys. Rev. **52**, 138 (1937).

Appendix

Proof that for small pressures the weakening is a linear function of the scattering pressure

1. *Weakening without scattering.* We consider a rectangular intensity distribution in the undeflected beam (see Fig. 4). The number of molecules contained in a strip of the width ds is $I_0 ds$. Assuming a magnetic split-up into two components, these molecules produce in the deflected beam at the position $s=0$ an intensity of

$$dI = \frac{I_0}{2} \cdot e^{-c^2/\alpha^2} \frac{c^2}{\alpha^2} d\frac{c^2}{\alpha^2} = \frac{I_0}{2} e^{-y} dy,$$

where $y = s_\alpha/s = c^2/\alpha^2$. The total intensity for $s=0$ is

$$I = 2\frac{I_0}{2}\int_{s_{\alpha/a}}^{\infty} e^{-c^2/\alpha^2} \frac{c^2}{\alpha^2} d\frac{c^2}{\alpha^2} = I_0 \int_{s_{\alpha/a}}^{\infty} e^{-y} y dy = I_0\left(1+\frac{s_\alpha}{a}\right) e^{-s_\alpha/a}.$$

2. *Weakening with scattering.* If the beam passes the distance l through scattering gas, the measured intensity I_0' will be smaller than I_0; the intensity of the molecules with the velocity c being weakened by the factor e^{-l/λ_c}. The mean free path λ_c is here an unknown function of the velocity c and the scattering pressure p. We make now the assumption, which should be valid always, that λ_c is proportional to $1/p$ and write $\lambda_c = \lambda_c{}^0/p$. Concerning $\lambda_c{}^0$ we assume only that it increases with c. Then we have

$$I' = 2\frac{I_0}{2}\int_{s_{\alpha/a}}^{\infty} e^{-(l/\lambda_c{}^0)p} e^{-c^2/\alpha^2} \frac{c^2}{\alpha^2} d\frac{c^2}{\alpha^2}.$$

Being interested only in the limit of I' for small values of p we may replace $e^{-(l/\lambda_c{}^0)p}$ by $1-(l/\lambda_c{}^0)p$. In practice this means that the weakening by the scattering should not be too large. Very slow molecules for which $\lambda_c{}^0$ is so small that $(l/\lambda_c{}^0)p$ is not small any more compared to one are so few that the error due to the replacement of $e^{-(l/\lambda_c{}^0)p}$ by $1-(l/\lambda_c{}^0)p$ is negligible. We have, therefore, for the intensity with field

$$I' = I_0\left[\int_{s_{\alpha/a}}^{\infty} e^{-c^2/\alpha^2} \frac{c^2}{\alpha^2} d\frac{c^2}{\alpha^2} - p\int_{s_{\alpha/a}}^{\infty} \frac{l}{\lambda_c{}^0} e^{-c^2/\alpha^2} \frac{c^2}{\alpha^2} d\frac{c^2}{\alpha^2}\right]$$

and without field

$$I_0' = I_0\left[\int_0^{\infty} e^{-c^2/\alpha^2} \frac{c^2}{\alpha^2} d\frac{c^2}{\alpha^2} - p\int_0^{\infty} \frac{l}{\lambda_c{}^0} e^{-c^2/\alpha^2} \frac{c^2}{\alpha^2} d\frac{c^2}{\alpha^2}\right].$$

Hence

$$\frac{I'}{I_0'} = \frac{I - p\int_{s_{\alpha/a}}^{\infty} (l/\lambda_c{}^0) e^{-c^2/\alpha^2} (c^2/\alpha^2) d(c^2/\alpha^2)}{I_0 - p_0 \int_0^{\infty} (l/\lambda_c{}^0) e^{-c^2/\alpha^2} (c^2/\alpha^2) d(c^2/\alpha^2)}$$

and for small values of p

$$\frac{I'}{I_0'} = \frac{I}{I_0}\left\{1 + p\left[\frac{1}{I_0}\int_0^{\infty} e^{-c^2/\alpha^2} \frac{c^2}{\alpha^2} d\frac{c^2}{\alpha^2} - \frac{1}{I}\int_{s_{\alpha/a}}^{\infty} \frac{l}{\lambda_c{}^0} e^{-c^2/\alpha^2} \frac{c^2}{\alpha^2} d\frac{c^2}{\alpha^2}\right]\right\}$$
$$= \frac{I}{I_0}(1+Cp).$$

A similar proof can be given for every point of the deflection curve.